Thermochimica Acta, 155 (1989) 135–149
Elsevier Science Publishers B.V., Amsterdam – Printed in The Netherlands

THE EFFECT OF EXPERIMENTAL VARIABLES ON THE MECHANISM OF THE OXIDATION OF PYRITE. PART 2. OXIDATION OF PARTICLES OF SIZE 90–125 μm

J.G. DUNN and G.C. DE

School of Applied Chemistry, Curtin University of Technology, Perth, W. Australia (Australia)

B.H. O'CONNOR

School of Physics and Geosciences, Curtin University of Technology, Perth, W. Australia (Australia)

(Received 28 March 1989)

ABSTRACT

The oxidation of pyrite of particle size 90–125 μm has been studied by simultaneous thermogravimetry–differential thermal analysis (TG–DTA). Partially oxidised samples were characterized by qualitative and quantitative X-ray diffraction (XRD) and scanning electron microscopy (SEM). The first weight loss, of 4%, occurred at 425–435 °C, and was associated with a weak exotherm. XRD analysis indicated 11% hematite present at 453 °C, with 86% pyrite unreacted. The SEM micrographs of samples heated to 453 °C were visually identical to those of unreacted pyrite, although analysis by energy dispersive X-ray spectrometry showed some rim oxidation. Between 450 and 515 °C there was a gradual weight loss of 55%, with an associated exothermic drift. The SEM micrographs revealed a pyrite core surrounded by a thick product coating. By 520 °C, 75% hematite was present as determined by XRD, with 16% pyrite remaining. The next weight loss, of 30%, occurred between 515 and 535 °C, and was coincident with the major exothermic peak observed. The hematite content increased to 89% by 550 °C, and no unreacted pyrite was detected. There was significant porosity apparent in the core of the particles. The final weight loss of 11% occurred above 565 °C. No DTA response was evident. Increasing the heating rate between 2.5 and 40 °C min^{-1} increased the third weight loss at the expense of the second. A similar effect was noted on changing the atmosphere from air to oxygen.

A comparison of the oxidation of pyrite of particle size < 45 and 90–125 μm has been made. The effects of changing the particle size, heating rate and atmosphere are discussed. Depending on the conditions chosen, one of the three following mechanisms of reaction operates: (i) slow combustion, controlled by oxygen diffusion; (ii) pyrolytic decomposition of pyrite and oxidation of the resulting pyrrhotite; and (iii) ignition. The TG–DTA records show distinct differences according to the prevailing mechanism.

INTRODUCTION

In a previous publication, we have reported on the oxidation of pyrite of particle size < 45 μm over a range of experimental variables [1]. Scanning

0040-6031/89/$03.50

electron microscopy (SEM) and quantitative and qualitative X-ray diffraction (XRD) techniques were used to examine particles at various stages of oxidation. At a heating rate of 2.5 °C min^{-1} in air, the major reaction is the direct conversion of pyrite to hematite in the temperature range 420–490 °C. At 505 °C, only 10% pyrite remained unreacted, with the formation of 65% hematite. The deficit of 25% was assigned to a ferric sulphate phase, which is formed simultaneously with the hematite, but which decomposes between 550 and 610 °C with the formation of more hematite. The reaction occurs via a shrinking core model. The oxide/sulphate coatings formed on the exterior of the particles are quite protective and the rate of oxidation is slow.

Increasing the heating rate and the oxygen partial pressure affected the reaction mechanism, and in a pure oxygen atmosphere at the fastest heating rate of 40 °C min^{-1}, the pyrite ignited. This produced a thermogravimetry–differential thermal analysis (TG–DTA) record which had one major weight loss and one major exothermic peak between 475 and 500 °C. No further reactivity was evident above 500 °C.

This paper reports on the results obtained in a similar study carried out on pyrite particles in the size range 90–125 μm.

EXPERIMENTAL

Full details of the characterization techniques have been described [1]. All work was carried out with the same sample of pyrite from the Dominican Republic as was used in the previous study.

RESULTS AND DISCUSSION

The pyrite sample was oxidised under a variety of conditions. Three sets of experiments were performed:

(a) heating the sample in air at 2.5 °C min^{-1}. The products at various stages of oxidation were isolated and examined by SEM and XRD, using a similar strategy to that adopted previously [1].

(b) changing the heating rate between 2.5 and 40 °C min^{-1}.

(c) changing the atmosphere from air to oxygen.

Pyrite heated in air at 2.5 °C min^{-1}

A typical TG–DTA result for the 90–125 μm pyrite particles is shown in Fig. 1.

To identify and estimate the phases formed during the oxidation reaction, samples were heated to temperatures of 453, 520 and 550 °C. The products were cooled rapidly and examined by qualitative and quantitative XRD. The

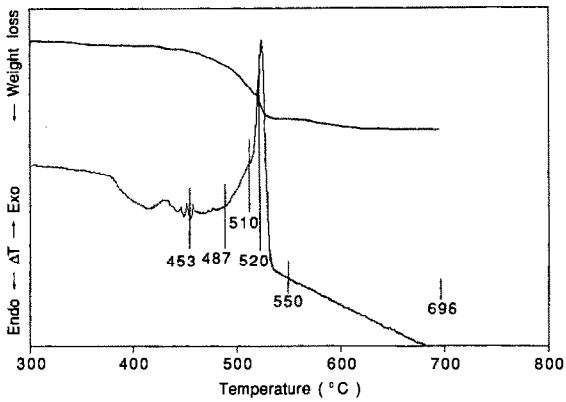

Fig. 1. TG–DTA trace of 90–125 μm particles of pyrite heated at 2.5 °C min^{-1} in air. Temperatures at which oxidised samples were taken for analysis are indicated by vertical lines.

qualitative assessment indicated that pyrite and hematite accounted for all lines in the XRD pattern. However, the increasing deficit with temperature between the two detected phases and 100% indicates that at least one other reaction is simultaneously taking place. This phase has not been identified by XRD, perhaps because of its low crystallinity. The results for quantitative analysis on the intermediate products are presented in Table 1.

To study the behaviour of individual particles at elevated temperatures, further samples were prepared under the same conditions as those for the XRD analysis at the temperatures indicated in Fig. 1. SEM micrographs of representative particles are shown in Fig. 2. Iron and sulphur were determined quantitatively by X-ray analysis at certain points on the particle by use of the SEM in the spot mode. Particles of pyrite were used as internal standards. Each particle was analysed at the rim and the centre. From these data the ratio of iron : sulphur was calculated and then the sulphur value normalized relative to iron.

TABLE 1

Weight per cent of the phases measured by XRD during the oxidation of pyrite (90–125 μm) at elevated temperatures

Sample temperature (°C)	Phase composition (%)		Deficit (%)
	Pyrite	Hematite	
453	86±2	11±3	3±5
520	16±2	75±3	9±5
550	0±3	89±4	11±7

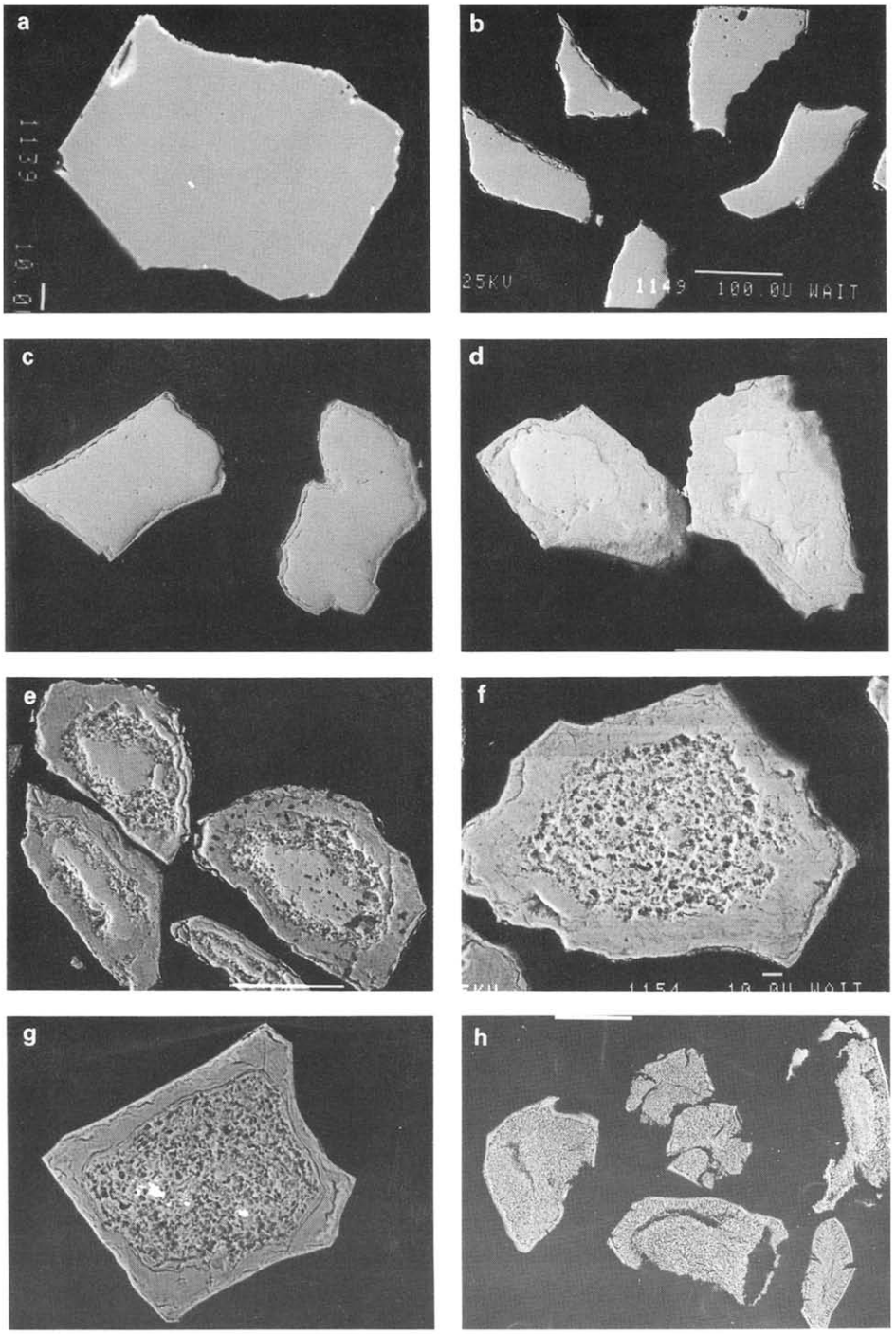

Fig. 2. SEM micrographs of 90–125 μm particles of pyrite heated at 2.5 °C min^{-1} in air to various temperatures and then cooled rapidly to room temperature: (a) unreacted pyrite; (b) 30–453 °C; (c) 30–487 °C; (d) 30–510 °C; (e) 30–520 °C; (f) 30–550 °C; (g) 30–696 °C; and (h) 30–700 °C, but heated at 40 °C min^{-1}.

The pyrite sample, which has been previously characterized [1], has a purity greater than 99%. An SEM micrograph of a typical unreacted pyrite particle is shown in Fig. 2a, and reveals a relatively smooth cross-section. Minor variations in the stoichiometric composition of the unreacted pyrite were evident from quantitative analysis, but the iron : sulphur ratios were on average 1 : 2. The composition of a single particle was uniform over the cross-section as revealed by scans across the surface.

The TG curves show four distinct weight loss regions. The weight loss calculations are based on the total weight loss between 400 and 700 °C, because of the conversion of pyrite to hematite, being 100%. The first loss occurs at temperatures between 425 and 435 °C and is quite minor, being typically 4%. Associated with this weight loss is a small exotherm between 420 and 440 °C. The XRD results indicate 11% hematite being present in the sample heated to 453 °C with 86% pyrite unreacted. The 3% deficit may reflect the presence of a small amount of sulphate. A comparison of the micrograph of an unreacted particle with that of the particle heated to 453 °C (Fig. 2b) reveals that no observable change has occurred. However, quantitative analysis showed small variations in reaction. Some particles showed no reaction, and both rim and centre analysed as FeS_2. Other particles showed significant reaction at the rim. This emphasizes the random nature of reaction initiation in these particles. The weight loss and the small exotherm can be assigned to the direct oxidation of pyrite to hematite. Sulphate formation tends to be slow and the associated exothermic effect is usually spread over a large temperature range so that it is too weak to be observed.

The major oxidation reaction occurs in the temperature region 450–515 °C. This is supported by both the TG and XRD results. The former technique shows a gradual weight loss of 55% in this temperature range, and the latter method indicates the presence of 75% hematite with only 16% pyrite remaining at 520 °C. The deficit of 9% is again attributed to the formation of an iron sulphate phase. However the DTA record shows an exothermic drift, which is particularly apparent between 490 and 515 °C, rather than a well defined peak. This is surprising in view of the highly exothermic nature of the oxidation of pyrite. The micrographs of the particles heated to 487 °C and above reveal a significant extent of oxidation. In general, quantitative SEM analyses showed that each particle consists of a rim of hematite surrounding an unreacted pyrite core. The thickness of the oxide rim is observed to increase with increase in the exposure time of the sample up to 510 °C. For example, Fig. 2c shows that particles heated to 487 °C (14 min after hematite was first detected at 453 °C) have an oxide rim of thickness of approximately 6 μm whilst particles heated to 510 °C (i.e. after 23 min) have a rim thickness of between 9 and 38 μm (Fig. 2d).

The thickness of the coating may account for the lack of a major exotherm. It has been shown for pyrite particles of < 45 μm that the

coatings are quite protective [1]; therefore, oxygen diffusion through the coating will be relatively slow, and hence the rate of oxidation will be slow. This will produce a broad peak. However before this peak can be fully expressed, the next reaction commences. The exothermic drift and the weight loss are again attributed to the direct oxidation of pyrite to hematite.

The next weight loss is 30% and occurs over a narrow temperature range of 515–535 °C. Associated with this is the major exothermic peak. At the end of this reaction the hematite content has increased from 75 to 89%, with the deficit being allocated to the sulphate phase. For particles heated between 510 and 520 °C, porosity is observed for the first time between the product rim and the unreacted pyrite core (Fig. 2e). Continued heating produces more porosity at the expense of the pyrite core. A porous interior within a rim of product phase is observed to be the general feature of the cross section of the particles heated to 550 (Fig. 2f) and 696 °C (end product, Fig. 2g). The porous region was found to have an iron : sulphur ratio of 1 : 0.02, and thus is essentially a zone of complete oxidation. At 550 °C and above, very little sulphur was detected in any of the particles by SEM.

It is apparent that the large particles (90–125 μm size fraction) require long time periods for oxidation to take place via oxygen diffusion, because at temperatures up to 515 °C there is still a significant quantity of pyrite remaining in the inner core of the particle. The thickness of the oxide film inhibits the oxygen diffusion process. As the sample is heated beyond 520 °C, pyrolytic decomposition of pyrite to pyrrhotite occurs with the evolution of sulphur. This reaction has been demonstrated by heating the Dominican pyrite sample in the TG–DTA apparatus in a nitrogen atmosphere at 2.5 °C min^{-1}. An endothermic effect and a weight loss were evident between 520 and 600 °C. The evolution of sulphur vapour creates porosity within the particles, as was observed using SEM. This porosity has a similar appearance to that shown by the particles heated in air (Fig. 2e–f). In air, the increase in the internal sulphur vapour pressure within the particle possibly causes additional channels to be formed in the oxide coating. The sulphur vapour is also readily oxidised in the gas phase near the surface of the particle. Hence the mechanism of this process is:

(1) $FeS_2 = FeS + S$ and evolution of sulphur outwards from the particle.

(2) Highly exothermic oxidation of sulphur in the gas phase.

(3) Rapid diffusion of oxygen into the particle interior and oxidation of freshly formed pyrrhotite.

The newly formed pyrrhotite is in a highly active state with a large surface area, so again the oxidation reaction is rapid. Thus, all of these reactions are rapid and controlled by the rate at which the pyrite decomposition step occurs. This view is supported by the highly porous structure of the cross-section of typical particles represented by the SEM micrographs shown in Fig. 2, e–g.

As the gas phase reaction (2) is highly exothermic, some particle heating is expected and actually observed in the temperature record of the DTA trace. The increase in particle temperature causes further pyrolytic decomposition, and so the overall reaction approaches an ignition mechanism. Indeed this reaction satisfies most of the criteria for an ignition reaction [2,3], in that: a very intense DTA peak and a sharp weight loss are observed; the reaction occurs over a small temperature range; and one of the reactions occurs in the gas phase.

At 2.5 °C min^{-1}, the weight loss corresponding to this reaction is only 30% of the total weight loss. Hence this intense peak is produced by the oxidation of about 0.55 mg of the total mass of 1.8 mg. The energetic nature of pyrite ignition compared with the slow oxidation is obvious.

The final weight loss is of the order of 11%. This occurs in the temperature region of 565–620 °C, and is associated with the decomposition of an iron sulphate phase. There is no endothermic peak detected as a result of this minor decomposition reaction.

Effect of heating rate

Figure 3 shows the effect of changing the heating rate from 2.5 to 40 °C min^{-1} on the TG–DTA curves for samples of pyrite in air.

The small low temperature peak shifts to higher temperatures with increase in heating rate, and eventually merges with the major exotherm at a heating rate of 40 °C min^{-1}. The major exotherm also shifts to higher temperatures, and occurs over an increasing temperature range.

An increase in heating rate altered the relative weight losses. As the heating rate increased, the first weight loss did not change significantly. However, the second weight loss decreased to 23% and remained at about this value at 20 and 40 °C min^{-1}, whilst the third weight loss increased with increasing heating rate. Above 10 °C min^{-1} this weight loss was about 55%.

Hence an increase in heating rate enhanced the third reaction, that is the pyrolytic decomposition of pyrite. At the faster heating rates the amount of time available for oxygen diffusion inwards through the protective coating is reduced. This decreases the direct conversion of pyrite to hematite, and increases the amount of unreacted pyrite which then remains to be pyrolytically decomposed.

The quantity of sulphate formed decreased with increase in heating rate.

Effect of atmosphere

The use of an oxygen atmosphere instead of air to oxidise pyrite caused some changes to the reactions (Fig. 4).

At 2.5 °C min^{-1}, the TG–DTA curves were similar to those obtained in air (Fig. 1). However, beyond 2.5 °C min^{-1}, the small exotherm before the

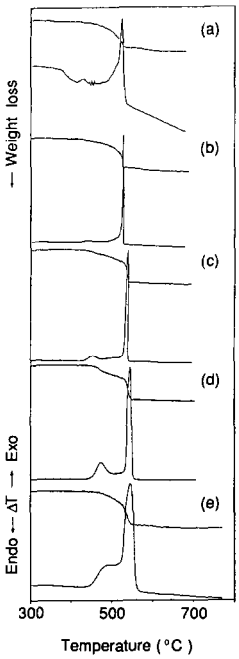

Fig. 3. TG–DTA traces of 90–125 μm particles of pyrite heated at various rates in air, with DTA sensitivities in parentheses (μV): (a) 2.5 °C min^{-1} (50); (b) 5 °C min^{-1} (100); (c) 10 °C min^{-1} (100); (d) 20 °C min^{-1} (200); and (e) 40 °C min^{-1} (500).

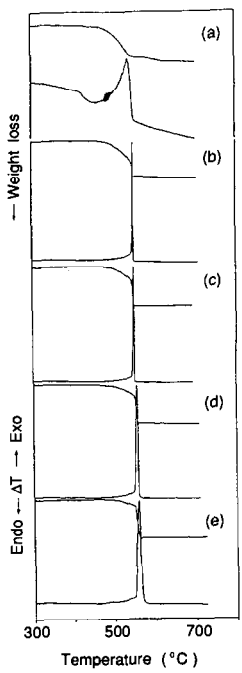

Fig. 4. TG–DTA traces of 90–125 μm particles of pyrite heated at various rates in oxygen, with DTA sensitivities in parentheses (μV): (a) 2.5 °C min^{-1} (100); (b) 5 °C min^{-1} (200); (c) 10 °C min^{-1} (200); (d) 20 °C min^{-1} (500) and (e) 40 °C min^{-1} (500).

main exotherm was absent except for the sample heated at 40 °C min^{-1}. The major exotherm and weight loss were sharp. As the heating rate increased, both these effects spread over increasing temperature intervals. A similar effect was noted in air (see Fig. 3).

A combination of heating rate and an oxygen atmosphere also had an effect on the relative extents of oxidation for the different reactions. In air at 2.5 °C min^{-1}, the weight loss associated with the very intense DTA peak was about 30%, and this increased to 57% at a heating rate of 40 °C min^{-1}. In oxygen, this weight loss at slower heating rates was not very different, but increased more rapidly as the heating rate increased. At 40 °C min^{-1}, the weight loss was 80%. The combined effect was thus to increase the quantity of unreacted pyrite available for pyrolytic decomposition, rather than direct oxidation.

A group of the particles from the sample heated to 700 °C at 40 °C min^{-1} in an oxygen atmosphere were examined using SEM. A view of the cross section of the group is shown in Fig. 2h. It is observed that the internal structure of each particle is highly porous, and is surrounded by a relatively thin oxide coating of about 5 μm thickness. There is considerable fracturing apparent, suggesting that the increase in the partial pressure of sulphur vapour as the pyrite decomposes is sufficient to break the particles. The morphology is quite different from that of the particles heated to 696 °C at 2.5 °C min^{-1}, and the latter are less porous and have much thicker oxide rims (compare Figs. 2g and 2h). These results support the time dependency of the reaction, with the faster heating rate enabling less oxygen diffusion, and so less rim oxidation and less oxidation of pyrite. Beyond 520 °C, the very rapid decomposition of pyrite causes a rapid increase in the activity of the sulphur vapour, which then exerts sufficient internal pressure to cause rupture of some of the particles.

COMPARATIVE EFFECTS OF EXPERIMENTAL VARIABLES ON THE OXIDATION OF PYRITE

The oxidation of pyrite has been studied whilst varying the particle size, heating rate and oxygen concentration. All three variables had a significant influence on the TG–DTA curves obtained.

Effect of particle size

The effect of particle size on the TG–DTA results was studied using < 45 μm and 90–125 μm sized particles. The results are presented in Fig. 5 for pyrite heated at 2.5 °C min^{-1} in air. Figure 5a is reproduced from ref. 1. It is obvious that the results are very different for the two fractions. Because of this, more experiments were carried out at a heating rate of 10 °C min^{-1} in

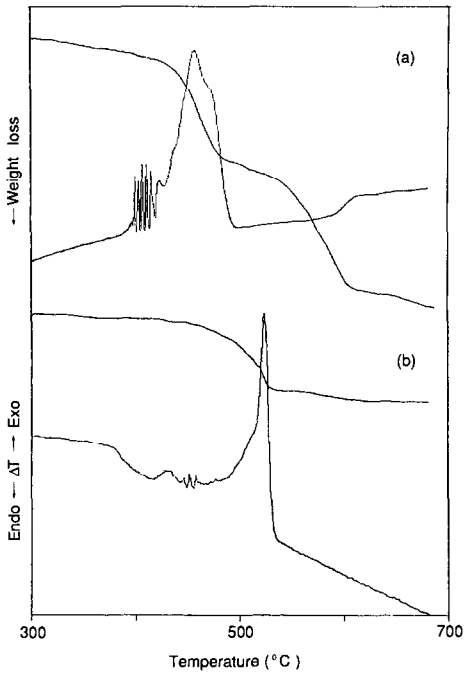

Fig. 5. TG–DTA traces of pyrite heated in air at 2.5 °C min^{-1}, showing the effect of particle size, DTA sensitivity 50 μv in each case: (a) particle size < 45 μm; (b) particle size 90–125 μm. Note: Fig. 5a is reproduced from ref. 1.

air with two additional fractions between 45 and 90 μm. These results are presented in Fig. 6. Both sets of results at 2.5 and 10 °C min^{-1} show similar trends, demonstrating that the effect is reproducible and not affected by the differing heating rates. The particle size effect is particularly dramatic for the DTA curve, with the disappearance of peaks and the emergence of new peaks at other temperatures.

With small (< 45 μm) particles, the DTA record (Fig. 5a) shows a multiple peaking effect around 400 °C, followed by a double peak commencing at 420 °C and complete by approximately 490 °C. These peaks shift in temperature as well as intensity with increase in particle size. For the largest particle size (90–125 μm) there are three peaks (Fig. 5b). The first is observed between 420 and 440 °C and represents a small exothermic effect. This is followed by an exothermic drift in the temperature range 450–515 °C which, in turn, is succeeded by a sharp intense peak between 515 and 535 °C. These observed changes are sufficiently significant to suggest changes in the course of oxidative transformation due to change in particle size. This suggestion is supported by the SEM results.

Fundamentally, the small and large particles differ in two major ways. Firstly the small particles have a much greater surface area to mass ratio than the larger particles. For this reason, small pyrite particles have a large

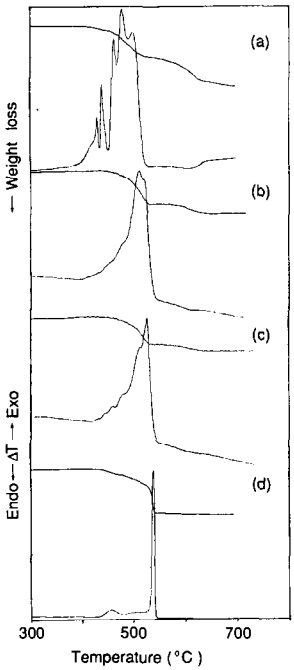

Fig. 6. TG–DTA traces of pyrite heated in air at 10 °C min^{-1}, showing the effect of particle size DTA sensitivity 200 μv in all cases: (a) < 45 μm; (b) 45–74 μm; (c) 74–90 μm; and (d) 90–125 μm.

pyrite–oxidant interfacial area available for oxidation, and tend to react at a faster rate compared with the large particles. Secondly the distance required for oxygen diffusion into the particle is less for the small particles than large particles. Therefore less time is required to completely oxidise a small particle relative to a large one.

These arguments can be used to explain the differences between the two sets of particles. At a heating rate of 2.5 °C min^{-1}, the small particles have sufficient time to be almost completely oxidised by 490 °C, with the major reactions being the direct oxidation of pyrite to hematite, and simultaneous formation of a sulphate species. Under similar reaction conditions, the 90–125 μm particles still contain a majority of unreacted pyrite at 490 °C, and significant quantities at 510 °C (see Fig. 2, c and d). Above 515 °C, further reaction takes place by a different mechanism. This is evident from a comparison of the SEM micrographs of the < 45 μm particles (Fig. 2, ref. 1) with those of the 90–125 μm particles (Fig. 2). The 90–125 μm particles heated to 520 °C and above (Fig. 2, e–g) contain a hematite rim around a porous interior whilst no porosity is observed at all in the corresponding SEM micrographs of < 45 μm particles. Hence the reaction that gives the major exotherm for the larger particles is the decomposition of pyrite to pyrrhotite with the evolution of sulphur vapour, which accounts for the

porosity of the particles, followed by the oxidation of the pyrrhotite and sulphur. This effect is readily evident in the experiments involving a heating rate of 10 °C min^{-1}. The exotherm associated with the oxidation of pyrrhotite to hematite becomes increasingly prominent and well resolved as the particle size increases (see Fig. 6).

It is observed from the TG curves (Figs. 5 and 6) that the final weight loss, above 550 °C, diminishes as the particle size increases. It has been shown [4–8] that the final weight loss is associated with the decomposition of an iron sulphate phase to hematite. Thus an increase in particle size is found to decrease the formation of the iron sulphate. The TG evidence is supported by the XRD results, which show that the difference between the sum of the hematite and pyrite phases and 100% is 25% for the small particles (see Table 1, ref. 1), and 11% for the large particles (Table 1, this paper). The formation of sulphate is the result of the reaction between newly formed hematite and SO_3, and so the increased surface area available for the small particles gives better reaction opportunities for the solid–gas interaction.

The multiple peaking effect at 420–440 °C has been shown to be associated with the oxidation of small particles of pyrite to hematite [9]. Hence the effect is absent from the TG–DTA record of the large particles.

Effect of heating rate

For the small particles, it has been shown that at heating rates of 2.5, 5 and 10 °C min^{-1}, only one major exotherm is evident which is complete by 490, 505 and 520 °C, respectively. At 20 and 40 °C min^{-1}, the strongest peak in the DTA trace commences at 520 °C and is not complete until about 550 °C (see Fig. 3 in ref. 1). The TG curve also changes below 540 °C, from a single weight loss at slower heating rates, to a two-stage process at the two higher heating rates. The first weight loss is still associated with the oxidation of pyrite to hematite, but the second is associated with the decomposition of pyrite to pyrrhotite with subsequent oxidation to hematite. This effect is evident for the large particles as well, with an increase in heating rate causing a shift towards the weight loss corresponding to the decomposition of pyrite to pyrrhotite.

The final weight loss above 550 °C, associated with the decomposition of a sulphate phase, decreases with increase in heating rate for both sets of particles. The formation of sulphate is enhanced by slow heating rates, which agrees with the known kinetics of that reaction [6].

These results further emphasise that oxygen diffusion into the particle is the rate-controlling step below 520 °C. Slow heating rates enhance direct oxidation of pyrite to either hematite and/or a sulphate phase, since sufficient time is available for the direct oxidation reaction to occur. Any factor that diminishes the time available for the reaction to occur, such as an

increase in heating rate, decreases the tendency for direct oxidation. At faster heating rates the reaction shifts, for both sets of particles, towards the mechanism controlled by the pyrolytic decomposition of pyrite.

Effect of atmosphere

For the small particles, an increase in oxygen concentration had a marked effect on the number of small narrow exotherms observed in the temperature range 400–460 °C. This effect has been discussed elsewhere [9]. The most dramatic effect of an increase in oxygen concentration is the tendency to promote ignition of the particles at faster heating rates. The effect was pronounced for the small particles at a heating rate of 40 °C min^{-1}.

CONCLUSIONS

The oxidation of pyrite is very susceptible to the experimental conditions chosen. Changing the particle size, heating rate and oxygen concentration caused major differences to appear in the TG–DTA records. These differences can be attributed to changes in the reaction mechanism. Three reaction mechanisms have been identified, as exemplified by the three TG–DTA records shown in Fig. 7.

(1) Oxygen diffusion into the sulphide particle is the major cause of reaction and the rate-controlling step below 515 °C. Oxidation occurs via a shrinking core mechanism, with the increasing movement of the reaction front towards the centre of the particle. The oxide/sulphate coating formed is protective and inhibits the oxygen diffusion process. If sufficient time is allowed, small particles of < 45 μm will be completely oxidised by this mechanism. An example of this kind of reaction is shown in Fig. 7a. There are two oxidative reactions: the conversion of pyrite to hematite causing the first weight loss and the exothermic peaks; and the formation of sulphate, which is not detected by either the TG or DTA techniques. The weight gain due to sulphate formation is masked by the simultaneous weight loss caused by the formation of the hematite.

Direct oxidation to hematite is encouraged by small particle size, faster heating rates and an air atmosphere, whilst sulphate formation is favoured by small particle size, slow heating rates and an oxygen atmosphere.

(2) Under conditions that do not give complete oxidation of pyrite by 515 °C, the mechanism changes to one in which the rate is controlled by the pyrolytic decomposition of pyrite to pyrrhotite with sulphur evolution. The evolved sulphur produces considerable porosity within the particle which assists in the rapid oxidation of the pyrrhotite to hematite. Large particles, faster heating rates and an oxygen atmosphere promote this mechanism. An example is shown in Fig. 7b. All exotherms and weight losses below 515 °C

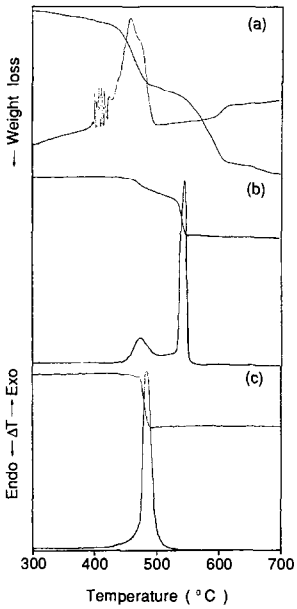

Fig. 7. TG–DTA traces of the oxidation of pyrite resulting from three different reaction mechanisms: (a) particle size $< 45\ \mu m$, heating rate $2.5\,^{\circ}C\ min^{-1}$, air, DTA sensitivity 50 μv; (b) particle size 90–125 μm, heating rate $20\,^{\circ}C\ min^{-1}$, air, DTA sensitivity 500 μv; and (c) particle size $< 45\ \mu m$, heating rate $40\,^{\circ}C\ min^{-1}$, oxygen, DTA sensitivity 500 μv. Note: Fig. 7, a and c are reproduced from ref. 1.

are assigned to the direct oxidation of pyrite to hematite, and above 515 °C the first weight loss and exotherm are assigned to the formation of hematite via the pyrrhotite intermediate.

(3) The third mechanism operates under conditions which are vigorous enough to cause the particles to ignite. This requires that the particles be heated at a sufficiently fast rate that heat generated by the initial oxidation at the surface of the particle is adsorbed by the particle rather than by the surrounding environment. This leads to particle self-heating, which causes the particle temperature to exceed the pyrolytic decomposition temperature of pyrite. Sulphur is evolved which oxidises rapidly in the gas phase, and this causes further pyrite decomposition. The reaction is self-sustaining and complete by 500 °C. Only one major exotherm and weight loss are evident (see Fig. 7c). This mechanism is encouraged by small particles, fast heating rates and an oxygen atmosphere.

ACKNOWLEDGEMENTS

One of us (G.C.D.) is grateful to the People's Republic of Bangladesh and Janangirnagar University for permission to pursue studies at Curtin Univer-

sity, and the Australian Development Assistance Bureau for financial support. We also thank Mr. I. Sills (Applied Chemistry) for technical support, Mr. A. Van Reissen (Applied Physics) for the provision of the SEM results, and Mr. L.C. Hammond and Mr. N. Kempt (Applied Physics) for measuring the XRD data.

REFERENCES

1 J.G. Dunn, G.C. De and B.H.O'Connor, Thermochim. Acta, 145 (1989) 115–130.
2 J.G. Dunn, S.A.A. Jayaweera and S.G. Davies, Proc. Aust. Ints. Min. Metal., 290(4) (1985) 75.
3 J.G. Dunn, S.G. Davies and L.C. Mackey, Proc. Aust. Ints. Min. Metal., in press.
4 C.M. Earnest, Thermochim. Acta, 75 (1984) 219.
5 F.R.A. Jorgensen and F.J. Moyle, Metal Trans., 12B (1981) 9.
6 A.C. Banerjee, P. Rangaswamy and S. Sood, in W. Hammenger (Ed.), Thermal Analysis, Birkhauser Verlag, Basel, 2 (1980) 241.
7 J.R. Schoor and J.O. Everhart, J. Am. Ceram. Soc., 52(7) (1969) 351.
8 F. Paulik, J. Paulik and M. Arnold, J. Ther. Anal, 31 (1986) 145.
9 J.G. Dunn, G.C. De and P.G. Fernandez, Thermochim. Acta, 135 (1988) 267.